Journal of Renewable Materials

Tech Science Press

DOI: 10.32604/jrm.2024.049948 Published Online: 03 April 2024

ARTICLE

Adhesion of Technical Lignin-Based Non-Isocyanate Polyurethane Adhesives for Wood Bonding

Jaewook Lee[1], Byung-Dae Park[1,*] and Qinglin Wu[2]

[1]Department of Wood and Paper Science, Kyungpook National University, Daegu, 41566, Korea

[2]School of Renewable Natural Resources, Louisiana State University, Baton Rouge, LA, 70806, USA

[*]Corresponding Author: Byung-Dae Park. Email: byungdae@knu.ac.kr

Received: 23 January 2024 Accepted: 27 February 2024

ABSTRACT

Lignin is the most abundant aromatic natural polymer, and receiving great attention in replacing various petroleum-based polymers. The aim of this study is to investigate the feasibility of technical lignin as a polyol for the synthesis of non-isocyanate polyurethane (NIPU) adhesives to substitute current polyurethane (PU) adhesives that have been synthesized with toxic isocyanate and polyols. Crude hardwood kraft lignin (C-HKL) was extracted from black liquor from a pulp mill followed by acetone fractionation to obtain acetone soluble-HKL (AS-HKL). Then, C-HKL, AS-HKL, and softwood sodium lignosulfonate (LS) were used for the synthesis of technical lignin-based NIPU adhesives through carbonation and polyamination and silane as a cross-linker. Their adhesion performance was determined for plywood. FTIR spectra showed the formation of urethane bonds and the reaction between lignin and silane. The NIPU adhesives prepared with C-HKL showed the highest adhesion strength among the three lignin-based NIPU adhesives. As the silane addition level increased, the adhesion strength of NIPU adhesives increased whereas formaldehyde emission decreased for all NIPU adhesives prepared. These results indicate that NIPU adhesives based on technical kraft lignin have a great potential as polyol for the synthesis of bio-based NIPU adhesives for wood bonding.

KEYWORDS

Technical lignin; non-isocyanate polyurethane; wood adhesives; adhesion strength; formaldehyde emission

1 Introduction

Polyurethane (PU) is one of the widely used polymers and was first synthesized with aliphatic and aromatic isocyanates by German chemists Wurtz and Hoffman in 1849. PU has been widely used in numerous applications owing to its versatility and affordable replacement of scarce materials [1,2]. However, several risks and problems with isocyanate monomers have been steadily raised. First, diisocyanate is most commonly synthesized via the toxic phosgene route (Fig. 1). Additionally, owing to the electrophilicity of isocyanate, it exhibits considerably high reactivity with water and other chemicals [3]. Furthermore, the recycling and disposal of expired isocyanate PU remain challenging [4].

As shown in Fig. 2, PU is generally formed via the reaction of diisocyanate synthesized through the phosgene route with a polyol [5]. The high risk of the phosgene route and the low sustainability of the materials have led to the development of new PU synthetic routes.

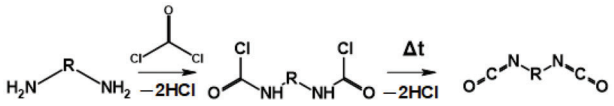

Figure 1: Phosgene route for synthesizing diisocyanate

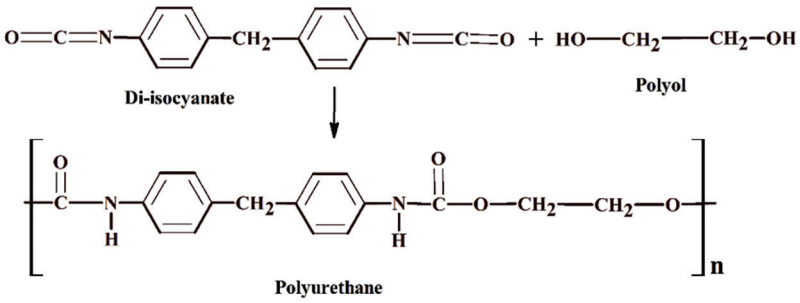

Figure 2: Mechanism of PU synthesis using diisocyanate and polyol

The first advanced attempt was conducted by excluding conventional materials, commonly referred to as non-isocyanate PU (NIPU) method. Oligomers terminated with carbonate-modified 5-membered cyclic carbonate successfully formed hydroxy urethane bonds in reaction with diamine [6]. Many studies have been conducted to improve the function of NIPU, and significant improvements have been found in the mechanical strength [7–10], fire retardancy [8,11,12], and thermal stability [11,13–15] of NIPU itself, as well as adhesion performance of wood composites [13,14,16–18]. Advanced NIPUs must be prepared with superior materials with economic and environmental benefits. Dimethyl carbonate (DMC) is a suitable solvent that can be used in carbonation [19,20]. DMC allows better control of spontaneous crosslinking reactions compared to epoxide groups and can also be obtained from renewable sources such as glycerin or CO_2 [21]. Additionally, no toxicity has been identified by contact or inhalation (Merck's index). NIPU research with DMC with controllable reactivity and safety has advanced considerably [7,16,22–25]. The hydroxy urethane bond formed by reacting with the primary amine is more robust than other types of amines (secondary and tertiary amines). It may be formed at a relatively low temperature (about 70°C) [26]. Additionally, the mechanical properties and chemical resistance of the synthesized NIPU are the best [27]. Hexamethylenediamine (HMDA) has the best potential among primary amines and is therefore being adopted in several NIPU studies [7,13,14,16,17,25,28,29].

Meanwhile, lignin [9,10,18,30–33], tannin [8,11–14,22–24,29,34], saccharides [11,16], plant oil [35], and soy protein [28] are examples of bio-polyols that can form the framework of the NIPU. Ingredients except lignin and tannin were excluded because of the disadvantage of having to compete with the food industry. As one of the most abundant forest product biomass on the earth, the use of lignin, which has yet to be given a straightforward industrial use, should be presented. Lignin is a phenolic polymer formed by oxygen radical polymerization of three basic monolignols. The oxygen radicals of monolignols exhibit different resonance structures, and they combine to form complex crosslinking bonds [36], an important aspect that promotes research on lignin utilization. In order to further increase the endless availability of lignin, lignin fractionation using solvents that increase the reactivity of lignin and obtain various chemical properties may be attempted. Fractionated lignin exhibits various molecular weights and polydispersity index (PDI) and acquires new properties [37–40]. Due to repeated modifications and advances in lignin, its commercialization has reached a visible level, and recently, cellulose/lignin composite films with high water resistance have also been invented [41].

Synthesis of NIPU from lignin was performed based on the polyaddition of carbonate and amine described previously. On the other hand, some studies have led to carbonation through epoxy-based materials, catalysts, and CO_2 fixation at high pressure instead of directly using factory-processed carbonate as a carbonation solvent [30,42]. CO_2 fixation is a reasonably exciting achievement, but the toxicity of epoxy-based materials such as epichlorohydrin (ECH) and the composition of a high-pressure environment for CO_2 fixation are challenges to be solved. The method attempted to overcome this problem is the procedure for oxyalkylation and carbonation of lignin hydroxyl groups using non-toxic carbonate. Sternberg and Pilla synthesized 100% bio-based carbon-containing NIPU foam with crude softwood kraft lignin, non-toxic carbonate, and fatty acid-based diamine [9]. In another study, NIPU with lignosulfonate as a bio-polyol was synthesized [31]. However, these procedures are still more complex than the simple polyaddition processes of DMC and HMDA. Saražin synthesized NIPU adhesives through a coreaction of organosolv lignin (OL) with DMC and HMDA [18]. The adhesion performance of particle boards prepared with synthesized adhesives met the criteria.

On the other hand, no research has been conducted on the procedure for synthesizing NIPUs through a multi-addition process using DMC and HMDA by technical lignins such as hardwood kraft lignin (HKL) and softwood sodium lignosulfonate (LS). Moreover, hydroxyl groups in hydroxy urethane bonds present throughout the NIPU structure improve adhesion and resistance to organic solvents at the expense of improved water uptake [15]. Nevertheless, research on NIPU synthesis to develop adhesives and confirm adhesion performance has been limited. Therefore, this study aims to investigate the feasibility of technical lignin as bio-polyol for the synthesis of NIPU adhesives through lignin carbonation and polyamination, and by characterizing their properties and determining their adhesion performance.

2 Materials and Methods

2.1 Materials

HKL was extracted from black liquor from a pulp mill (Moorim P&P Co., Ltd., Ulsan, Korea).

In addition, LS obtained by treating black liquor from sodium sulfite pulping mill (Yunjinglinzhi Co., Ltd., Kunming, China) was used without further treatment. Fig. 3 displays three technical lignin samples used in this study. Sulfuric acid, 20 wt% sodium hydroxide, acetone, pyridine, and acetic anhydride were purchased from a local supplier (Duksan Pure Chemicals Co., Ltd., Ansan, Korea). Tetrahydrofuran (THF), purchased by Sigma Aldrich (St. Louis, MS, USA), was used as a mobile phase for gel permeation chromatography (GPC). In addition, dimethyl carbonate (DMC, 99 wt%) and (3-glycidyloxypropyl)trimethoxysilane (GPTMS) were purchased from Sigma Aldrich (St. Louis, MS, USA). Hexamethylenediamine (HMDA), acetic acid, ammonium acetate, and acetylacetone were purchased from a local supplier (Daejung Chemicals & Metals Co., Ltd., Siheung, Korea).

Figure 3: Photographs of lignin used in this work; crude-HKL (C-HKL, left), acetone soluble-HKL (AS-HKL, middle), and LS (right)

2.2 Methods

2.2.1 Extraction and Acetone Fractionation of HKL

First, 350 mL of hardwood kraft pulping black liquor was placed into a reactor, and the pH of the solution was set to 9.0 using a 4 N aqueous sulfuric acid solution. Thereafter, the solution was stirred for 1 h at 70°C. The resulting suspension was filtered using a Büchner funnel and filter paper (No. 41, Whatman International Ltd., Maidstone, UK). Subsequently, the filtered solid was placed in the reactor. Afterward, 1000 mL of 2 wt% aqueous sulfuric acid solution was added per 100 g of the solid for washing, followed by filtration under the same conditions as in the previous step. Finally, the filtered solid was placed into the reactor, and 1000 mL of distilled water was added per 100 g of solid, followed by washing and filtration under the same conditions as those adopted in the previous steps. Thereafter, the filtered solid was dried at 60°C to obtain C-HKL powder. The dried C-HKL was washed with distilled water at room temperature for 2 h. The suspension was filtered with a Büchner funnel and filter paper (Whatman No. 41), and the solid was dried at 60°C for two days. The C-HKL was acetone fractionated to obtain AS-HKL and acetone insoluble-HKL (AI-HKL) according to the reported method [43].

2.2.2 Chemical Characterization of HKL

Attenuated total reflection-Fourier transform infrared (ATR-FTIR) spectroscopy (ALPHA-P, Bruker Optics GmbH, Ettlingen, Germany) was used to identify the aliphatic and phenolic hydroxyl groups of HKL as bio-polyol for NIPU adhesives. Prior to the analysis, HKL was heated using an oven at 105°C to remove moisture, and 32 scans were performed in the range of 400–4000 cm^{-1} with a resolution of 4 cm^{-1} for the minimum–maximum normalization of each sample spectrum.

A gel permeation chromatography (GPC, e2695, Waters Alliance, Milford, MA, USA) was used to measure the molecular weight and polydispersity of C-HKL, AS-HKL, and AI-HKL. Prior to measuring the molecular weight using GPC, three lignin samples were acetylated with pyridine and acetic anhydride under stirring. The acetylated lignin samples were filtered with a filter paper (Whatman 0.45 μm nylon membrane filter), and dried to obtain an acetylated lignin [44,45]. The lignin sample for GPC analysis was obtained by dissolving 2 mg of acetylated lignin in 1 mL of THF, followed by ultrasonication for 5 s and filtration with a 0.45 mm polytetrafluoroethylene syringe filter [46]. The polystyrene standard with a molecular weight of 1060 Da–2330 kDa was used. The molecular weight measurement using the GPC equipped with a refractive index (RI) detector was performed using a set of column ovens at 35°C and a set at a flow rate of 1 mL/min.

Elemental analysis was performed using an element analyzer (Flash 2000, ThermoFisher Scientific, Waltham, MA, USA) to confirm the changes in the elemental composition due to the acetone fraction of HKL. Prior to the analysis, the lignin specimen was sufficiently dried at 105°C [47]. For this test, 20 mg of a lignin specimen was placed into a device and burned in the presence of a catalyst at 950°C. The emitted gas was separated into a fixed phase column, and the gas composition was determined using a thermal conductivity detector (TCD).

The ash content was analyzed to confirm the changes in the ash content due to the acetone fractionation of HKL. The lignin used in the ash content test was prepared using 0.7 g of the specimen. The specimen weight was measured after completely removing moisture from lignin at 105°C using an oven, similar to the elemental analysis method. Thereafter, the specimen was placed in a crucible and burned at a temperature of 525°C ± 25°C for 4 h using a furnace. The ash content of kraft lignin was calculated using the weight ratio before and after combustion, as shown in Eq. (1).

$$Ash\ content\ (wt\%) = \frac{ash\ weight\ after\ combustion\ (g)}{lignin\ weight\ before\ combustion\ (g)} \times 100(\%) \quad (1)$$

2.2.3 Synthesis and Properties of NIPU Adhesives

Three lignin samples, C-HKL, AS-HKL, and LS, were used for the synthesis of NIPU adhesives through carbonation and polyamination, as reported [18]. The carbonation refers to the reaction of HKL and LS as bio-polyols with DMC to attach carbonate to aromatic and aliphatic hydroxyl groups of lignin. For the synthesis of HKL-NIPU, 25.9 wt% of HKL powder and 21.6 wt% of distilled water were poured into a 3-neck flask equipped with a reflux condenser. And 17.5 wt% of DMC was added into the reactor under stirring at 50°C for 40 min with a magnetic bar, then cooled at room temperature. For the synthesis of LS-NIPU adhesive, 26 wt% of LS powder and 32.6 wt% of distilled water were poured into a three-neck flask. And 26.4 wt% of DMC was added into the reactor under stirring 50°C for 40 min with a magnetic bar, then cooled to room temperature. The pH of NIPU adhesives prepared was measured immediately after the synthesis of adhesives, using a pH meter (SevenCompact S210, METTLER TOLEDO, Columbus, OH, USA). The solids content was determined by measuring the mass before and after drying 1 g of the sample at 105°C for 3 h. The viscosity of the samples was measured using a viscometer (DV-II +, Brookfield, Middleboro, MA, USA) with 82 spindle numbers at 20 rpm.

2.2.4 Chemical Characterization of NIPU Adhesives

ATR-FTIR spectra were analyzed for NIPU adhesives to confirm the formation of urethane bonds and silane reaction with lignin prepared by the same condition. Furthermore, differential scanning calorimetry (DSC) (Discovery 25, TA Instruments, New Castle, DE, USA) was used to confirm the peak related to the urethane bond through the thermal curing behavior of NIPU. Considering the solid content of the two adhesives, 8 mg–10 mg of HKL-NIPU and 18 mg–20 mg of LS-NIPU were sealed in a high-pressure capsule pan. The NIPU adhesives were scanned in the range of 0°C–200°C; the heating rate was 2.5, 5, 10, and 20°C/min; and the nitrogen flow rate was 50 mL/min. The reaction enthalpy and conversion (α) were calculated using the software installed in the DSC system (Universal Analysis 2000 V4.5A, TA Instruments, New Castle, DE, USA).

2.2.5 Adhesion Performance of NIPU Adhesives for Plywood

Plywood was manufactured using three Radiata pine veneers. The prepared NIPU adhesive was applied to the veneer without a hardener and extender. The three-ply plywood sample was prepared with a glue spread of 300 g/m^2 and a dimension of 300 mm × 300 mm × 6 mm. The plywood assembly was first cold pressed using an appropriate weight at room temperature for 15 min and subsequently hot pressed. Similar to those in previous studies [18], the hot press conditions in the preliminary test were a pressure of 1 MPa applied for 6 min at 200°C. However, owing to excessively high temperatures, all adhesives were evaporated before the sufficient permeation of the adhesive into the adherend, resulting in delamination. Among the two hot press conditions—9 min at 160°C and 8 min at 180°C—the latter condition comprising the newly modified pressing temperature and time was more beneficial. Therefore, the hot press conditions of this experiment were set to an applied pressure of 1 MPa for 8 min at 180°C after 15 min of cold pressing. Prior to further experiments, all samples were cured at room temperature for 24 h to stabilize the adhesive surface.

Tensile shear strength (TSS), wood failure (WF), and formaldehyde emission (FE) of plywood were measured according to Korean standards (KS F 3101 and KS M 1998). TSS was measured employing a universal testing machine (UTM, TX0044-Model-H50KS, Hounsfield, Redhill, UK) at a crosshead speed of 2 mm/min using 10 samples per one resin (dimension: 25 mm × 80 mm × 6 mm). For the FE test (KS M 1998, 24 h desiccator method), 12 FE samples (dimension: 50 mm × 150 mm × 6 mm) and 300 mL of H_2O were added to a desiccator and held at 20°C ± 2°C for 24 h. Subsequently, 25 mL of the water in the desiccator was added to a 100 mL Erlenmeyer flask. The mixed solution was then heated in a water bath at 65°C ± 2°C for 10 min and cooled to room temperature for 30 min in the dark. The FE of each

specimen was evaluated using an ultraviolet-visible spectrophotometer (OPTIZEN POP, KLAB Co., Ltd., Daejeon, South Korea) at a wavelength of 412 nm.

3 Results and Discussion

3.1 Extraction and Acetone Fractionation Yield of HKL

The yield and molecular weight of the extracted lignin increase in applied pH during extraction [48,49]. Therefore, the characteristics of lignin are substantially affected by the process conditions and additives used for pulping. Considering the various by-products of the pulping process, several methods for measuring the solid content (total dissolved solid method) in extracted lignin have been developed. Herein, the TAPPI/ANSI T 650 om-15 method was used to calculate the HKL yield. The calculated yield using Eqs. (2) and (3) of C-HKL is 19.63 wt%.

$$Recovery\ yield\ (wt\%) = \frac{Dried\ black\ liquor\ (g)}{Black\ liquor\ before\ drying\ (g)} \times 100(\%) \tag{2}$$

$$C{-}HKL\ yield\ (wt\%) = \frac{C{-}HKL\ after\ extraction\ (g)}{Black\ liquor\ for\ extraction\ (g) \times \frac{Recovery\ yield}{100}} \times 100(\%) \tag{3}$$

The yield of AS-HKL and AI-HKL obtained through acetone fractionation was calculated using Eqs. (4) and (5), respectively, as approximately 7:3, which is similar to the values obtained in previous studies [50].

$$AS{-}HKL\ yield\ (wt\%) = \frac{AS{-}HKL\ output\ (g)}{C{-}HKL\ input\ (g)} \times 100(\%) \tag{4}$$

$$AI{-}HKL\ yield\ (\%) = \frac{AI{-}HKL\ output\ (g)}{C{-}HKL\ input\ (g)} \times 100(\%) \tag{5}$$

3.2 FTIR Analysis of HKL

Functional groups in C-HKL, AS-HKL, and AI-HKL were characterized using ATR-FTIR spectroscopy. The spectra of all the extracted and acetone-fractionated HKL are shown in Fig. 4, and the wavenumber of each peak is listed in Table 1. The peak positions in the C-HKL and AS-HKL spectra, which were expected to be refined at a relatively similar level, were approximately similar, and the intensities of peaks corresponding to the functional groups in AI-HKL were different from those in other lignin spectra. However, peaks corresponding to new functional groups were not observed, which is consistent with the previous studies [48]. The peaks at 3358, 2917, 2848, 1705, 1596, 1511, 1459, 1422, 1323, 1268, 1211, 1110, 1088, 1033, and 826 cm^{-1} are typical peaks of kraft lignin [51–53]. The peaks of 2917 and 2848 cm^{-1} correspond to the C–H axis deformation of CH_2 and CH_3 in the aliphatic side chain, and the peaks at 1596, 1511, and 1422 cm^{-1} are associated with various skeletal vibrations of aromatic rings (C=C bonds). Furthermore, the peaks at 1268 and 1211 cm^{-1} correspond to the C–O bands associated with the guaiacyl and syringyl monomers of hardwood lignin, respectively. The peak of 3358 cm^{-1} is related to the aliphatic and aromatic (phenol) hydroxyl groups of lignin. The high reactivity and functionality of hydroxyl groups may play a significant role in the HKL-NIPU synthesis. Therefore, all lignin samples could function as bio-polyols for NIPU adhesives owing to the hydroxyl groups in lignin.

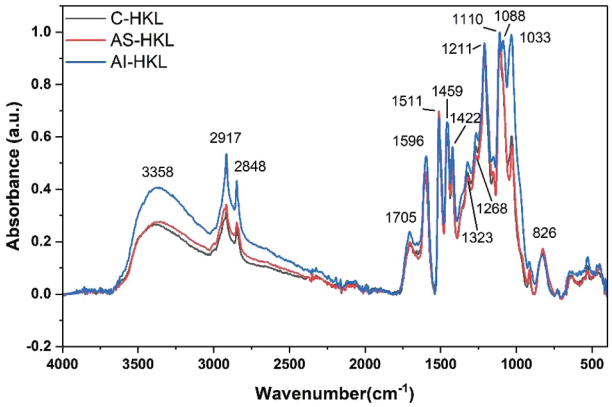

Figure 4: ATR-FTIR spectra of extracted or acetone-fractionated HKL samples

Table 1: Functional group assignment of each peak in the HKL spectra

Wavenumber (cm^{-1})	Functional group
3358	O–H bond
2917	C–H asymmetric stretching
2848	C–H symmetric stretching
1705	C=O symmetric/asymmetric stretching
1596, 1511	Aromatic skeletal vibration (C=C bond)
1459	Asymmetric flexural deformation of methyl and methylene groups
1422	In-plane deformation of C–H by aromatic ring stretching (C=C bond)
1323	Symmetric bending deformation of the methyl group
1268	C–O of syringyl ring
1211	C–O of guaiacyl ring
1110	C–C + C–O stretching
1088	C–O deformation of ester bonds
1033	Aromatic C–H in-plane deformation (G > S) + C–O deformation of primary alcohol
826	C–H out-of-plane of 2, 5, and 6 carbon of guaiacyl monomers

3.3 Molecular Weight Analysis of HKL

For molecular weight measurement, all HKL samples were acetylated according to the reaction, as shown in Fig. 5. ATR-FTIR spectra, shown in Fig. 6, confirm the acetylation of HKL samples. Table 2 presents the weight-average molecular weight (M_w), number-average molecular weight (M_n), and polydispersity index (PDI). The results were consistent with the values obtained from the black liquor procured from the same factory and subjected to the same extraction process [50]. The results confirmed that the molecular weight of AS-HKL was relatively low and had a narrow distribution range, showing potential as a polyol for NIPU synthesis [54–57]. By contrast, the molecular weight of AI-HKL was relatively high and a broad distribution range. These results are consistent with previous studies and suggest that AS-HKL comprise a fewer polymer molecules than that of AI-HKL [58].

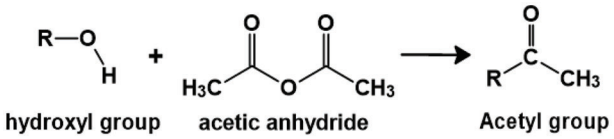

Figure 5: Acetylation of extracted and acetone-fractionated HKL

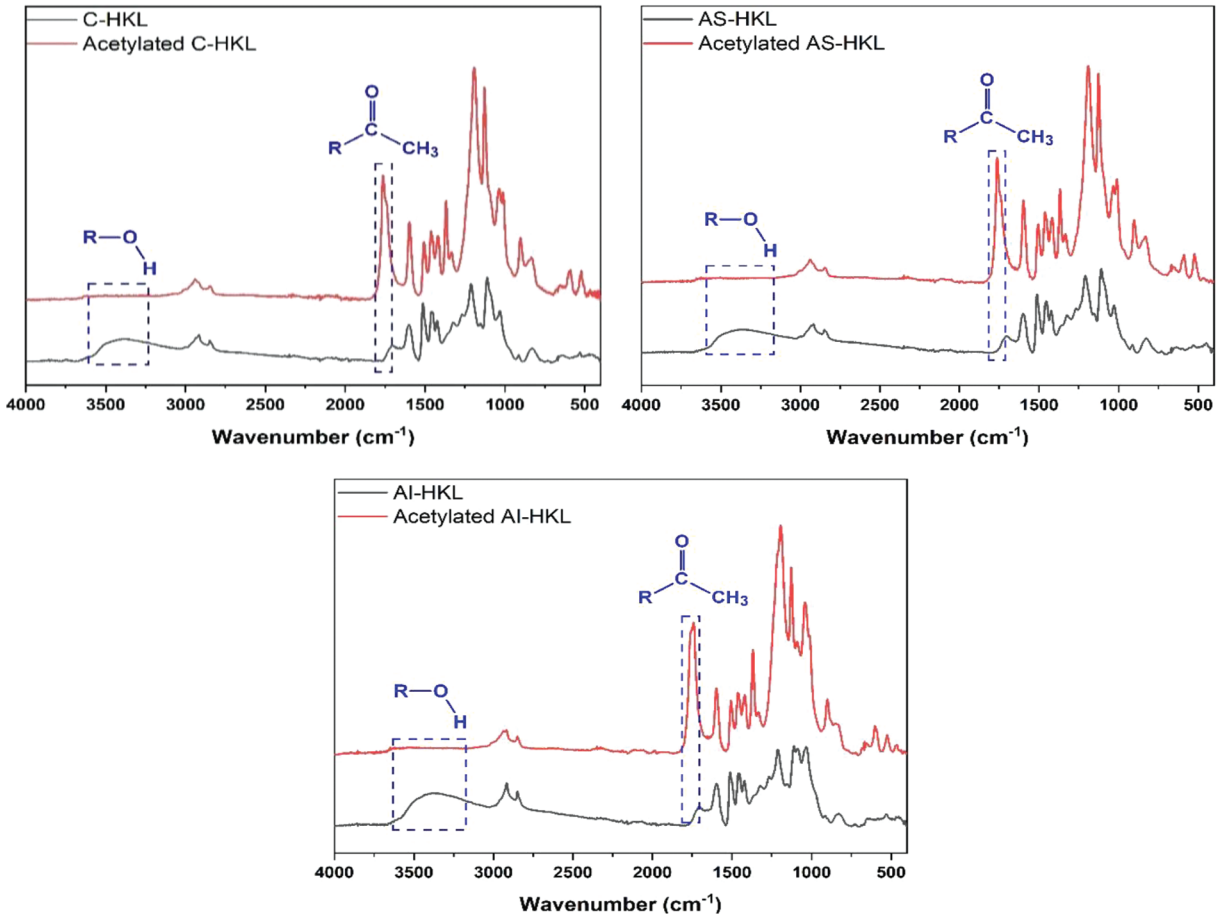

Figure 6: ATR-FTIR spectra of acetylated C-HKL, AS-HKL, and AI-HKL

Table 2: Molecular weights of HKL samples by GPC analysis

Lignin	M_w (g/mol)	M_n (g/mol)	PDI
C-HKL	4436	2441	1.82
AS-HKL	3270	2231	1.47
AI-HKL	13191	4238	3.11

3.4 Elemental and Ash Content Analysis of HKL

The elemental composition of the three lignin samples, C-HKL, AS-HKL, and AI-HKL, was analyzed via elemental analysis. The composition of the burned kraft lignin in the form of gas was detected using the

TCD. Table 3 lists the element composition, empirical formula, and ash content of C-HKL, AS-HKL, and AI-HKL. The elemental composition of AS-HKL and C-HKL were similar. In contrast, the carbon and oxygen contents of AI-HKL were significantly different from those of AS-HKL and C-HKL. The ash content of the three lignin samples was substantially lower than that obtained in other pulping processes, and high impurities remained in the order of AI-HKL, C-HKL, and AS-HKL [49,59]. The elemental composition of LS was similar to previous studies [60–63]. The high ash content (18.5 wt%) of LS was ascribed to a high content of metal ions in LS.

Table 3: Element composition and ash content of C-HKL, AS-HKL, and AI-HKL

Lignin	C (%)	H (%)	O (%)	N (%)	S (%)	Empirical formula	Ash content (%)
C-HKL	63.03	5.67	28.99	0.39	1.92	$C_{5.25}H_{5.62}O_{1.81}N_{0.03}S_{0.06}$	0.40
AS-HKL	63.81	5.72	28.30	0.29	1.88	$C_{5.31}H_{5.68}O_{1.77}N_{0.02}S_{0.06}$	0.06
AI-HKL	58.84	5.96	32.80	0.55	1.85	$C_{4.90}H_{5.91}O_{2.05}N_{0.04}S_{0.06}$	0.57

3.5 Physical Properties of NIPU Adhesives

Table 4 presents the pH, solids content, and viscosity of HKL-NIPU and LS-NIPU adhesives prepared. AI-HKL was not used for the synthesis of NIPU adhesives because of its insufficient yield for the NIPU synthesis. The pH of HKL-NIPU and LS-NIPU adhesives was approximately 10.5 and 9.6, respectively. This difference in pH values is due to the pH of bio-polyol and the composition of materials (lignin, DMC, and HMDA). Furthermore, as the silane content increased, the pH of adhesives slightly increased. The solid content of HKL-NIPU was higher than that of LS-NIPU, which was slightly different from those obtained in previous studies [18]. The solids content of all the adhesives increased with an increase in the silane content. In addition, LS-NIPU adhesive was hardened when 20% silane as a crosslinker was added. The most significant difference between the NIPU adhesives is observed for their viscosity (Table 4). The viscosity of HKL-NIPU adhesive was approximately 10 times higher than that of LS-NIPU. This is due to differences in the temperature during the polyamination of HKL-NIPU and LS-NIPU.

Table 4: Properties of NIPU adhesives prepared in this study

Lignin	Silane (wt%)	pH	Solid content (wt%)	Viscosity (mPas)
C-HKL	0	10.5	50.5	1,094
	10	10.6	56.4	2,440
	20	11.0	58.8	6,790
AS-HKL	0	10.6	50.7	764
	10	10.7	54.1	1,690
	20	10.5	59.0	3,955
LS	0	9.6	40.1	94
	10	9.6	42.0	105
	20	N/A*	N/A*	N/A*

Note: *N/A means not available.

3.6 FTIR Analysis of NIPU Adhesives

Figs. 7 and 8 show the reaction schemes of the NIPU adhesives based on HKL and LS, respectively, via carbonation and amination with HMDA to form urethane bonds. HMDA was added to DMC, cooled to 30°C, then stirred for 2 h at 90°C to form urethane bonds in HKL-NIPU adhesives. 15 wt% LS was added to carbonated intermediates in the reactor to cool to 30°C and then stirred for 2 h at 60°C to synthesize LS-NIPU adhesives. The polyamination temperature of LS-NIPU was set low because the crosslinking reaction rate was fast, and the adhesive was cured when the reaction was carried out at the same temperature as HKL-NIPU. In addition, two GPTMS addition levels (10% and 20% of the dry mass of NIPU) as a crosslinker were added to help cross-linking, leading to an improvement of the adhesion [18,64–67].

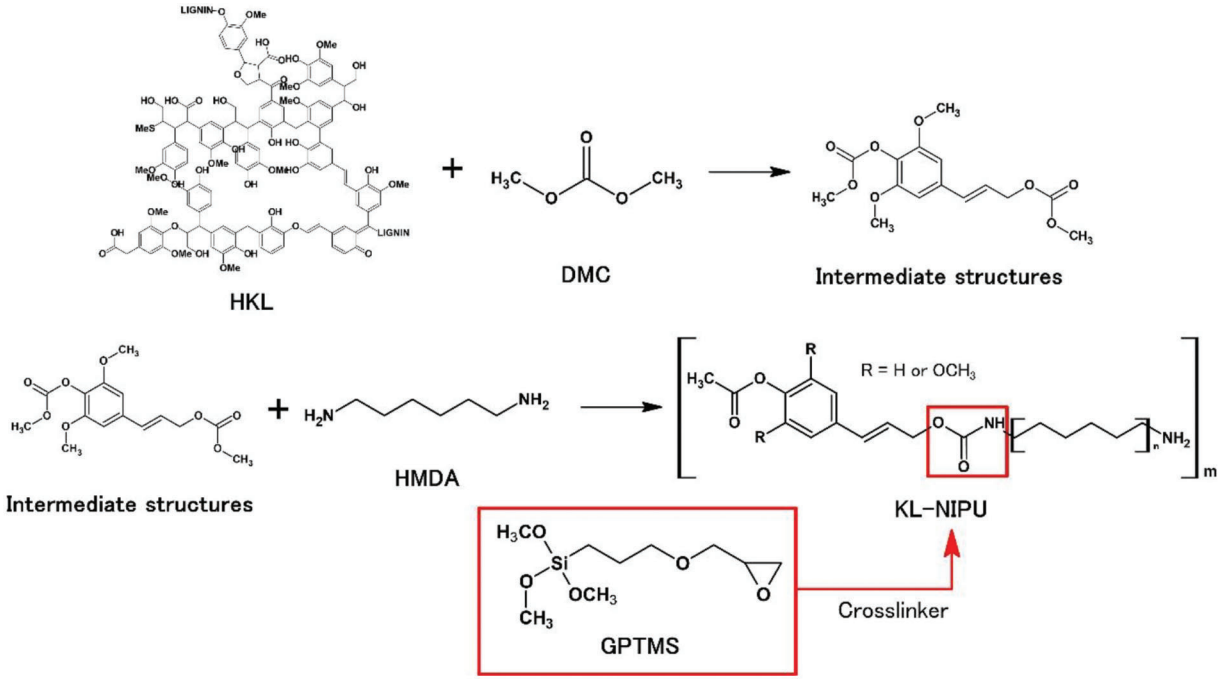

Figure 7: Reaction scheme of the synthesis of HKL-NIPU

The functional groups in NIPU were characterized using ATR-FTIR spectroscopy. Fig. 9 displays the NIPU spectra, and the assignment of each peak is presented in Table 5. The spectra of HKL-NIPU and LS-NIPU were slightly different. The common peaks in the spectra are as follows. Peaks associated with the C=O bond of the urethane bonding were observed at 1680 and 1531 cm^{-1}, which were not detected in lignin spectra (Fig. 4). Additionally, these peaks represent the NH–CO urethane structure [16,22,23,68]. Furthermore, the peak at 1259 cm^{-1} is related to the structure of NH–CO urethane, the amide structure of the urethane bond [16,23,68], and the epoxy group of silane [66]. The peaks of 2929, 2854, and 1460 cm^{-1} represent asymmetric stretching of the $–CH_2–$ chain of HMDA [18]. The peaks at 3310–3337 and 1033 cm^{-1} correspond to the hydrogen-bond stretching of aliphatic alcohol, and therefore, they represent side chains of lignin units. The presence of a broad peak at 3310–3337 cm^{-1} implies that the same amount of hydroxyl group as the urethane bond is newly formed rather than consumed by the reaction when the urethane bond of NIPU mainly forms in the free phenolic hydroxyl

group of lignin or C=C double bonds in the α and β bonds of lignin [18]. Additionally, when comparing the FTIR spectra of the HKL and NIPU, the width of the broad peak of the –OH group of 3100–3500 cm^{-1} in the HKL is considerably narrower in the NIPU. It is due to the evaporation of water during the crosslinking process and the condensation reaction between hydroxymethyl groups or hydroxymethyl groups and NH_2 groups [69]. The peak at 1033 cm^{-1} is also associated with the Si–O–C and Si–O–Si bonds in the silane crosslinker (GPTMS) [66]. The peak at 1116–1139 cm^{-1} is related to the epoxy group of GPTMS and the Si–O–C and Si–O–Si bonds caused by GPTMS [65]. The peak at 817 cm^{-1} is related to the Si–O–C bond caused by GPTMS and the Si–OH bond due to the hydrolysis of GPTMS [66,70].

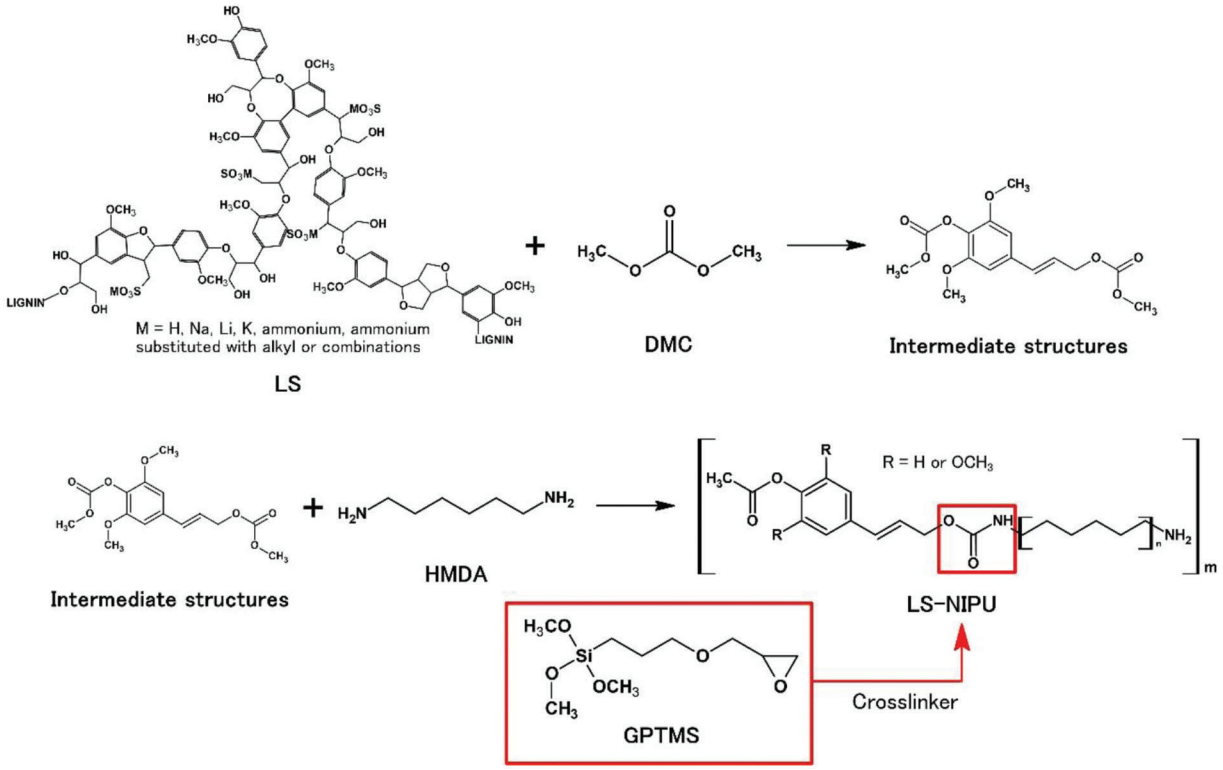

Figure 8: Synthesis mechanism of LS-NIPU

Next, the peaks detected in the HKL-NIPU or LS-NIPU spectrum are described. The small peak at 1510 cm^{-1} observed only in the LS-NIPU spectrum is associated with the C–H bending vibration (C=C bond) of $–CH_2–$ and $–CH_3$ of LS [59]. This observation implies that unreacted LS remained after carbonation and polyamination, which affected the adhesion performance. A peak at 1009 cm^{-1} associated with the silanol group (Si–OH) produced via GPTMS hydrolysis was observed in all HKL-NIPU spectra but was absent in the LS-NIPU spectrum. The prominent peak of LS-NIPU at 1034 cm^{-1} can be regarded as an overlapping peak, which masks the peaks corresponding to various functional groups overlapped with other peaks [18]. However, HKL-NIPU possesses better reaction activity between the crosslinker and NIPU in the absence of masking. Additionally, the peak at 1190 cm^{-1} is related to the Si–C bond of silane, which is present only in LS-NIPU [65]. ATR-FTIR spectroscopy confirmed that the urethane and silane bonds in the HKL-NIPU and LS-NIPU adhesives were formed at different levels.

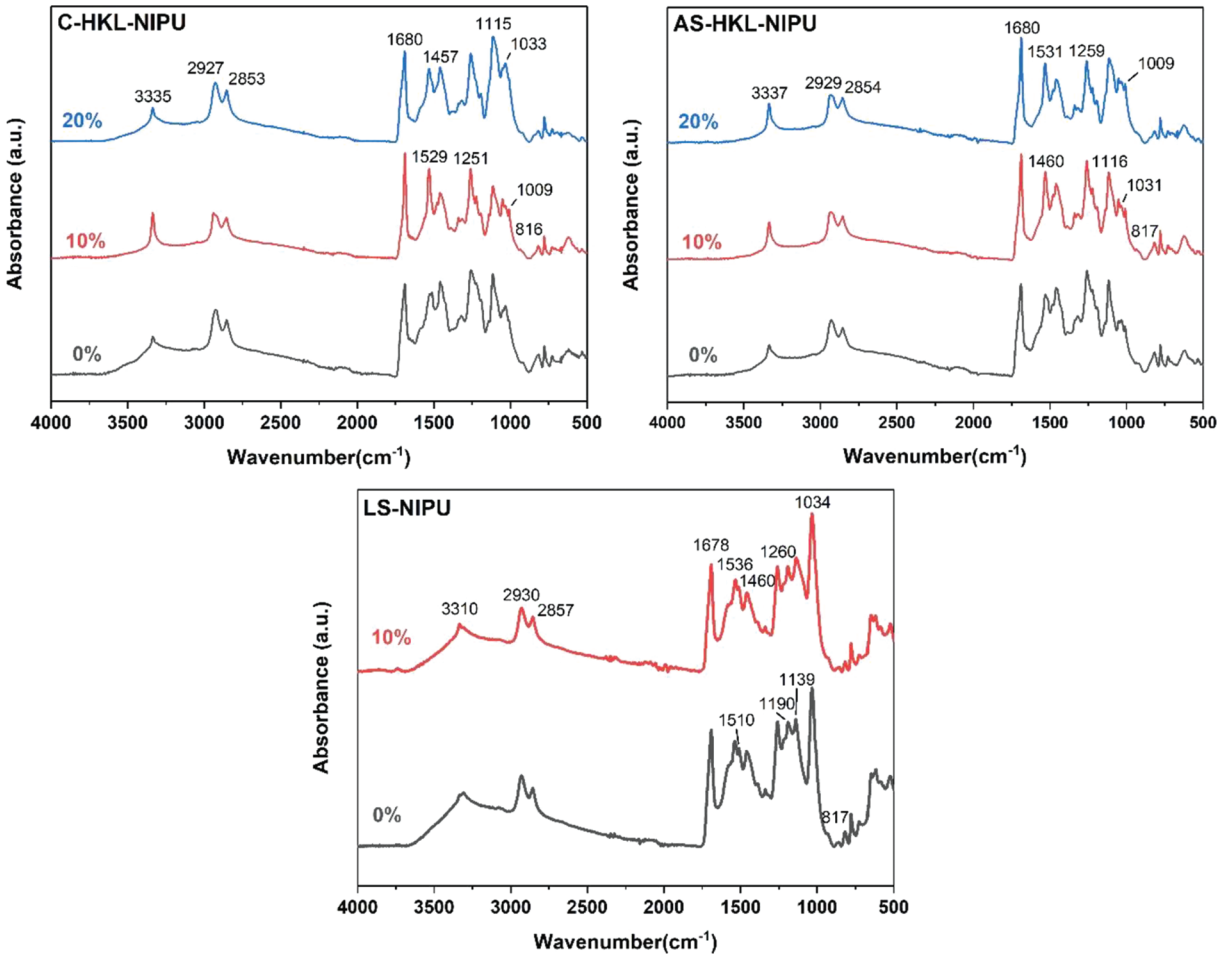

Figure 9: ATR-FTIR spectra of NIPU samples with different silane contents

Table 5: Functional group assignment of each peak in the NIPU spectra

Wavenumber (cm^{-1})	Functional group
3310–3337, 1033	Hydrogen bond stretching of aliphatic alcohol (side chain of lignin units) and Si–O–C and Si–O–Si bond of silane
2929, 2854, 1460	Asymmetric stretching of the $–CH_2–$ chain belonging to HMDA
1680, 1531	C=O bond and NH–CO of the urethane group
1510	C–H bending vibration of $–CH_2–$ and $–CH_3$ in LS (C=C bond)
1259	NH–CO urethane structure or amide group or epoxy group of silane
1190	Si–C of silane
1116–1139	Epoxy group of silane, and Si–O–C and Si–O–Si bond
1009	Silanol group (Si–OH) by hydrolysis of silane
817	Si–O–Si and Si–OH of silane

3.7 Thermal Curing Behavior of NIPU Adhesives

The thermal curing behavior of NIPU adhesives was characterized using DSC. Fig. 10 displays DSC thermograms of NIPU adhesive samples. For all adhesives, an exothermic peak corresponding to the urethane bond was observed for all NIPU adhesives. Furthermore, the onset temperature (T_{onset}) was approximately 50°C–60°C, which was similar to the T_{onset} of the exothermic peak due to the urethane bond of the NIPU adhesive [30,67]. Additionally, the glass transition temperature (T_g) of NIPU adhesives formed by adding HMDA during polyamination was the same as that observed in a previous study [30]. As presented in Fig. 11, the T_{onset}, T_g, and curing peak temperature (T_p) decreased after the addition of silane, which was consistent with the results of the previous study [67]. These results confirm that GPTMS aids in achieving complete curing and excellent bonding performance under the hot press. Furthermore, the exothermic peak observed for the curing of LS-NIPU was smaller than that detected for HKL-NIPU adhesives, confirming that the urethane binding activity of LS-NIPU was lower than that of HKL-NIPU. Therefore, DSC results confirmed the presence of the urethane bond in the NIPU adhesives and the adhesion performance of NIPU adhesives with the addition of the silane as a crosslinker.

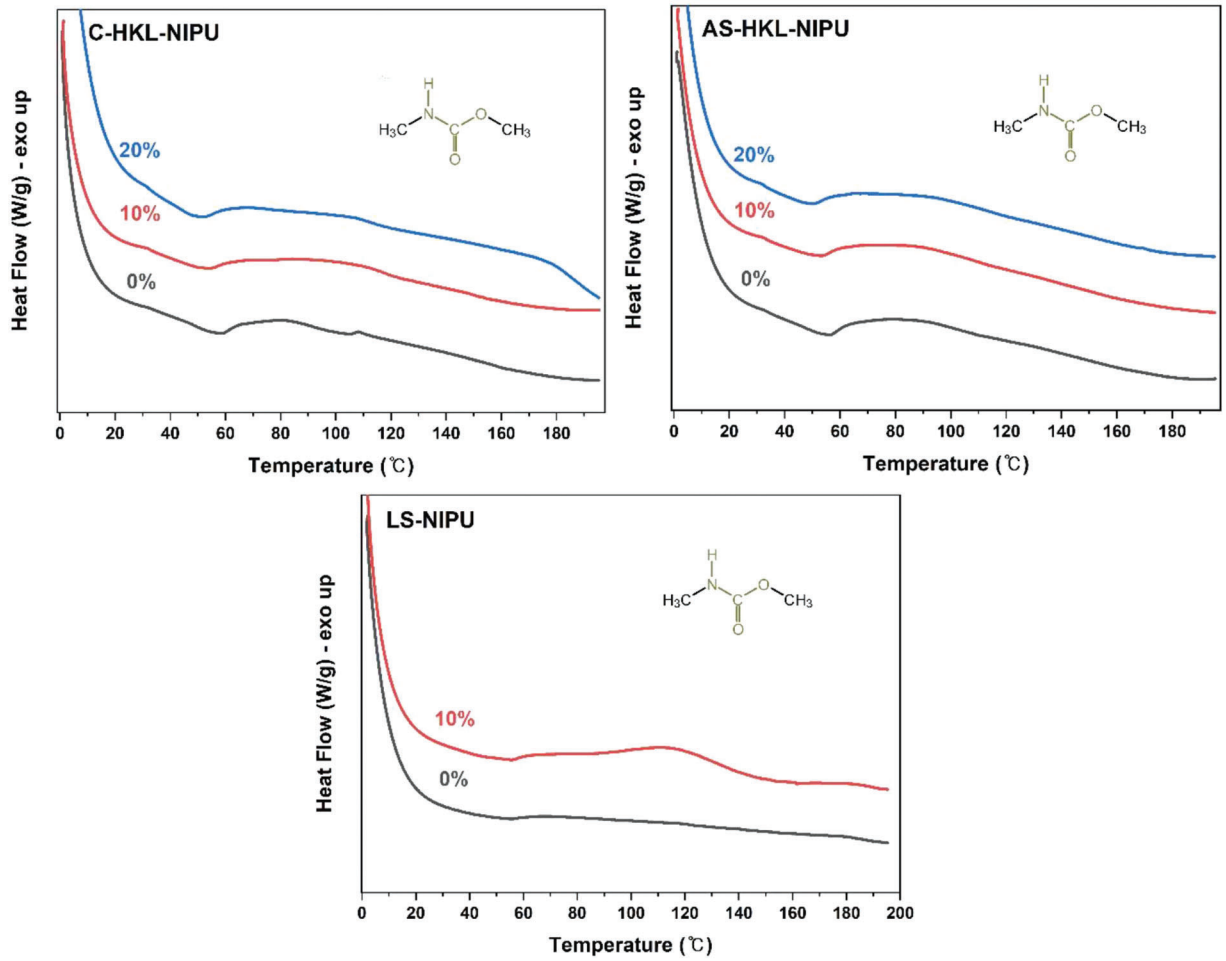

Figure 10: DSC thermograms of NIPU adhesives prepared

As shown in Fig. 11, the curing reaction of HKL-NIPU adhesives cure at lower temperatures than those of LS-NIPU adhesives. A significant increase in the viscosity of the adhesives with an increase in silane content is ascribed to the reaction of the aliphatic and aromatic hydroxyl groups of unreacted lignin with the epoxy group of silane and silicon [67].

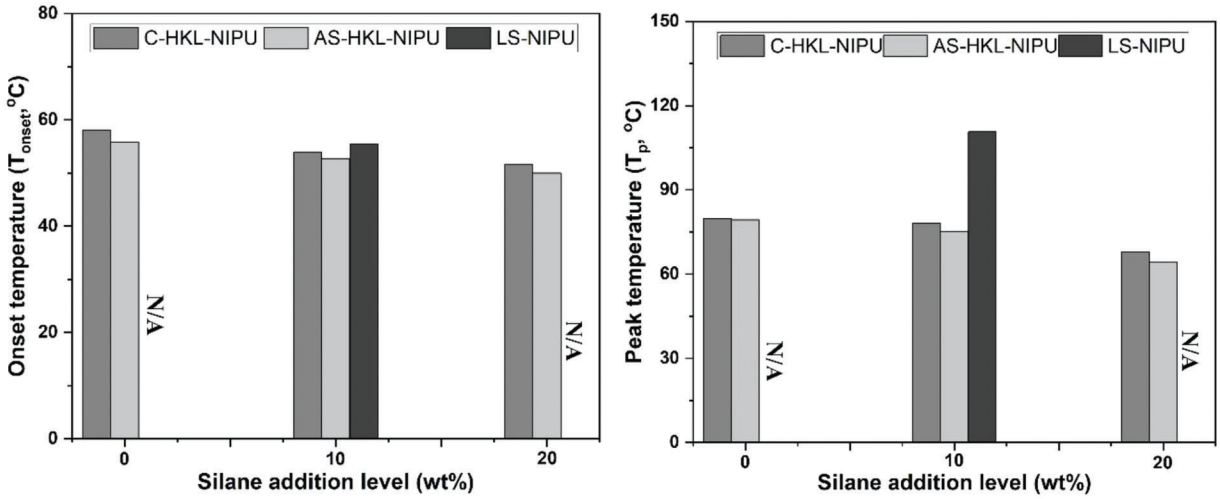

Figure 11: Onset and peak temperatures of NIPU samples at different silane levels. N/A means not available

3.8 Adhesion Performance of NIPU Adhesives for Plywood

Tensile shear strength (TSS), wood failure (WF), and formaldehyde emission (FE) of three-ply plywood bonded with the NIPU adhesives at different levels of silane addition are summarized in Fig. 12 and Table 6. All NIPU adhesives without GPTMS except the C-HKL-NIPU adhesives were delaminated and were not evaluated. FE of all NIPU adhesives was relatively low. TSS and WF increased for all NIPU adhesives with an increase in the GPTMS content, whereas FE slightly decreased. The C-HKL-NIPU adhesive exhibits the highest adhesion performance when the adhesion strength and FE of three NIPU adhesives are compared. A better adhesion performance of C-HKL-NIPU adhesives than those of AS-HKL-NIPU could be due to the higher molecular weight of C-HKL than that of AS-HKL, as shown in Table 2. In addition, LS-NIPU adhesive exhibits a lower adhesion performance than those of HKL-NIPU adhesives because LS-NIPU adhesives have relatively less urethane bonding, which is confirmed by an unreacted peak in the FTIR spectra of LS-NIPU adhesives. This was further supported by smaller urethane peaks in the DSC thermogram of LS-NIPU adhesives than those of the HKL-NIPU thermograms.

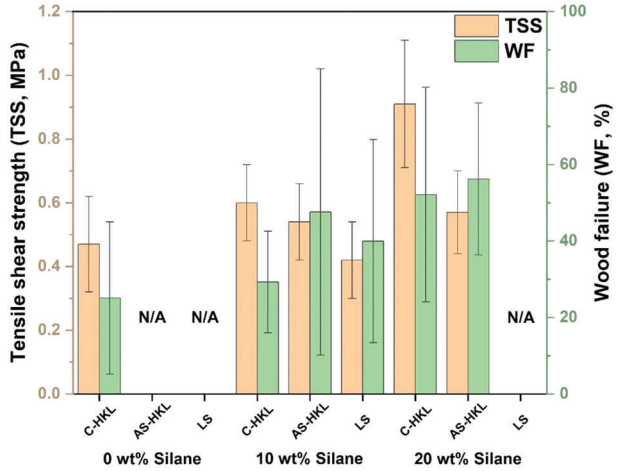

Figure 12: TSS and WF of plywood bonded with NIPU adhesives with different silane contents. N/A means not available

Table 6: FE results of NIPU adhesives with different silane contents

Lignin	Silane (wt%)	FE (mg/L)
C-HKL	0	0.06
	10	0.05
	20	0.01
AS-HKL	0	N/A*
	10	0.05
	20	0.01
LS	0	N/A*
	10	0.10
	20	N/A*

Note: *N/A means not available.

4 Conclusions

This study investigated three technical lignins as potential polyols for the synthesis of NIPU adhesives for wood bonding. Three technical lignin samples, such as C-HKL extracted from black liquor of hardwood kraft pulping mill, AS-HKL, and LS, were used for the synthesis of NIPU adhesives. These three technical lignins and NIPU adhesives for wood bonding were characterized with various analytical techniques such as elemental analysis, GPC, FTIR, and DSC as well as determining their adhesion strength of plywood. The GPC results show that AS-HKL possesses lower molecular weight and polydispersity than those of AI-HKL. FTIR spectra confirmed the presence of urethane and silane bonds in the NIPU adhesives prepared. The NIPU adhesives based on C-HKL showed the best adhesion strength among the NIPU adhesives based on AS-HKL, or LS. As the level of silane as a cross-linker increased, the adhesion strength was improved. And the formaldehyde emission was quite low compared with those of formaldehyde-based adhesives. These results indicate that technical lignin has great potential as polyols for the synthesis of NIPU adhesives for bonding wood.

Acknowledgement: The authors are grateful to Moorim P&P Co., Ltd., Ulsan, Korea and Yunjinglinzhi Co., Ltd., Kunming, China for the donation of black liquor of kraft pulping and LS from sodium sulfite pulping, respectively.

Funding Statement: This work was supported by the National Research Foundation (NRF) of Korea, and funded by the Korean Government (MSIT) (Grant No. RS-2023-00240043).

Author Contributions: Byung-Dae Park conceived and designed the experiments, and reviewed the paper. Jaewook Lee performed the experiment and wrote the paper. Byung-Dae Park acquired funding for this work. Qinglin Wu provided a critical review on the manuscript.

Availability of Data and Materials: Data is available upon request.

Conflicts of Interest: The authors declare that they have no conflicts of interest to report regarding the present study.

References

1. Petrović ZS, Wan X, Bilić O, Zlatanić A, Hong J, Javni I, et al. Polyols and polyurethanes from crude algal oil. J Am Oil Chem Soc. 2013;90:1073–8. doi:10.1007/s11746-013-2245-9.

2. Rajput SD, Hundiwale DG, Mahulikar PP, Gite VV. Fatty acids based transparent polyurethane films and coatings. Prog Org Coat. 2014;77(9):1360–8. doi:10.1016/j.porgcoat.2014.04.030.
3. Chipinda I, Stetson SJ, Depree GJ, Simoyi RH, Siegel PD. Kinetics and mechanistic studies of the hydrolysis of diisocyanate-derived bis-thiocarbamates of cysteine methyl ester. Chem Res Toxicol. 2006;19(3):341–50. doi:10.1021/tx050311t.
4. Włoch M, Datta J. Nonisocyanate polyurethanes. In: Thomas S, Datta J, Haponiuk J, Reghunadhan A, editors. Polyurethane polymers. Amsterdam: Elsevier; 2017. p. 169–202. doi:10.1016/B978-0-12-804039-3.00007-5
5. Six C, Richter F. Isocyanates, organic. Ullmann's Encycl Ind Chem. 2000;20:63–82. doi:10.1002/14356007.a14_611.
6. Rokicki G, Piotrowska A. A new route to polyurethanes from ethylene carbonate, diamines and diols. Polym. 2002;43(10):2927–35. doi:10.1016/S0032-3861(02)00071-X.
7. Xi X, Pizzi A, Gerardin C, Lei H, Chen X, Amirou S. Preparation and evaluation of glucose based non-isocyanate polyurethane self-blowing rigid foams. Polym. 2019;11(11):1802. doi:10.3390/polym11111802.
8. Zhao Y, Zhang Q, Lei H, Zhou X, Du G, Pizzi A, et al. Preparation and fire resistance modification on tannin-based non-isocyanate polyurethane (NIPU) rigid foams. Int J Biol Macromol. 2024;258:128994. doi:10.1016/j.ijbiomac.2023.128994.
9. Sternberg J, Pilla S. Materials for the biorefinery: high bio-content, shape memory Kraft lignin-derived non-isocyanate polyurethane foams using a non-toxic protocol. Green Chem. 2020;22(20):6922–35. doi:10.1039/D0GC01659D.
10. Quinsaat JEQ, Feghali E, van de Pas DJ, Vendamme R, Torr KM. Preparation of biobased nonisocyanate polyurethane/epoxy thermoset materials using depolymerized native lignin. Biomacromolecules. 2022;23(11):4562–73. doi:10.1021/acs.biomac.2c00706.
11. Chen X, Li J, Xi X, Pizzi A, Zhou X, Fredon E, et al. Condensed tannin-glucose-based NIPU bio-foams of improved fire retardancy. Polym Degrad Stab. 2020;175:109121. doi:10.1016/j.polymdegradstab.2020.109121.
12. Azadeh E, Chen X, Pizzi A, Gérardin C, Gérardin P, Essawy H. Self-blowing non-isocyanate polyurethane foams based on hydrolysable tannins. J Renew Mater. 2022;10(12):3217–27. doi:10.32604/jrm.2022.022740.
13. Chen X, Pizzi A, Fredon E, Gerardin C, Zhou X, Zhang B, et al. Low curing temperature tannin-based non-isocyanate polyurethane (NIPU) wood adhesives: preparation and properties evaluation. Int J Adhes. 2022;112:103001. doi:10.1016/j.ijadhadh.2021.103001.
14. Chen X, Essawy H, Wu H, Pizzi A, Fredon E, Gerardin C, et al. Mimosa tannin based NIPU wood adhesive with significant substitution of hexamethylenediamine using polyethyleneimine. Int J Adhes. 2024;128:103549. doi:10.1016/j.ijadhadh.2023.103549.
15. Blattmann H, Fleischer M, Bähr M, Mülhaupt R. Isocyanate- and phosgene-free routes to polyfunctional cyclic carbonates and green polyurethanes by fixation of carbon dioxide. Macromol Rapid Commun. 2014;35(14):1238–54. doi:10.1002/marc.201400209.
16. Xi X, Pizzi A, Delmotte L. Isocyanate-free polyurethane coatings and adhesives from mono- and di-saccharides. Polym. 2018;10(4):402. doi:10.3390/polym10040402.
17. Chen X, Pizzi A, Essawy H, Fredon E, Gerardin C, Guigo N, et al. Non-furanic humins-based non-isocyanate polyurethane (NIPU) thermoset wood adhesives. Polym. 2021;13(3):372. doi:10.3390/polym13030372.
18. Saražin J, Pizzi A, Amirou S, Schmiedl D, Šernek M. Organosolv lignin for non-isocyanate based polyurethanes (NIPU) as wood adhesive. J Renew Mater. 2021;9(5):881–907. doi:10.32604/jrm.2021.015047.
19. Annunziata L, Diallo AK, Fouquay S, Michaud G, Simon F, Brusson JM, et al. α, ω-Di (glycerol carbonate) telechelic polyesters and polyolefins as precursors to polyhydroxyurethanes: an isocyanate-free approach. Green Chem. 2014;16(4):1947–56. doi:10.1039/C3GC41821A.
20. Tundo P, Selva M. The chemistry of dimethyl carbonate. Acc Chem Res. 2002;35(9):706–16. doi:10.1021/ar010076f.
21. Besse V, Camara F, Voirin C, Auvergne R, Caillol S, Boutevin B. Synthesis and applications of unsaturated cyclocarbonates. Polym Chem. 2013;4(17):4545–61. doi:10.1039/C3PY00343D.

22. Thébault M, Pizzi A, Dumarçay S, Gerardin P, Fredon E, Delmotte L. Polyurethanes from hydrolysable tannins obtained without using isocyanates. Ind Crops Prod. 2014;59:329–36. doi:10.1016/j.indcrop.2014.05.036.
23. Thébault M, Pizzi A, Essawy HA, Barhoum A, van Assche G. Isocyanate free condensed tannin-based polyurethanes. Eur Polym J. 2015;67:513–26. doi:10.1016/j.eurpolymj.2014.10.022.
24. Thébault M, Pizzi A, Santiago-Medina FJ, Al-Marzouki FM, Abdalla S. Isocyanate-free polyurethanes by coreaction of condensed tannins with aminated tannins. J Renew Mater. 2017;5(1):21–9. doi:10.7569/JRM.2016.634116.
25. Xi X, Pizzi A, Gerardin C, Du G. Glucose-biobased non-isocyanate polyurethane rigid foams. J Renew Mater. 2019;7(3):301–12. doi:10.32604/jrm.2019.04174.
26. Camara F, Benyahya S, Besse V, Boutevin G, Auvergne R, Boutevin B, et al. Reactivity of secondary amines for the synthesis of non-isocyanate polyurethanes. Eur Polym J. 2014;55:17–26. doi:10.1016/j.eurpolymj.2014.03.011.
27. Figovsky OL, Shapovalov LD. Features of reaction amino-cyclocarbonate for production of new type nonisocyanate polyurethane coatings. Macromol Symp. 2002;187(1):325–32. doi:10.1002/1521-3900(200209)187:1%3C325::AID-MASY325%3E3.0.CO;2-L.
28. Chen X, Pizzi A, Xi X, Zhou X, Fredon E, Gerardin C. Soy protein isolate non-isocyanates polyurethanes (NIPU) wood adhesives. J Renew Mater. 2021;9:1045–57. doi:10.32604/jrm.2021.015066.
29. Azadeh E, Pizzi A, Gerardin-Charbonnier C, Gerardin P. Hydrolysable chestnut tannin extract chemical complexity in its reactions for non-isocyanate polyurethanes (NIPU) foams. J Renew Mater. 2022;11(6):2823–48. doi:10.32604/jrm.2023.027651.
30. Janvier M, Ducrot PH, Allais F. Isocyanate-free synthesis and characterization of renewable poly (hydroxy) urethanes from syringaresinol. ACS Sustain Chem Eng. 2017;5(10):8648–56. doi:10.1021/acssuschemeng.7b01271.
31. Mimini V, Amer H, Hettegger H, Bacher M, Gebauer I, Bischof R, et al. Lignosulfonate-based polyurethane materials via cyclic carbonates: preparation and characterization. Holzforschung. 2020;74(2):203–11. doi:10.1515/hf-2018-0298.
32. Kühnel I, Saake B, Lehnen R. A new environmentally friendly approach to lignin-based cyclic carbonates. Macromol Chem Phys. 2018;219(7):1700613. doi:10.1002/macp.201700613.
33. Salanti A, Zoia L, Mauri M, Orlandi M. Utilization of cyclocarbonated lignin as a bio-based cross-linker for the preparation of poly(hydroxy urethane)s. RSC Adv. 2017;7(40):25054–65. doi:10.1039/C7RA03416D.
34. Chen X, Xi X, Pizzi A, Fredon E, Zhou X, Li J, et al. Preparation and characterization of condensed tannin non-isocyanate polyurethane (NIPU) rigid foams by ambient temperature blowing. Polym. 2020;12(4):750. doi:10.3390/polym12040750.
35. Nohra B, Candy L, Blanco JF, Guerin C, Raoul Y, Mouloungui Z. From petrochemical polyurethanes to biobased polyhydroxyurethanes. Macromolecules. 2013;46(10):3771–92. doi:10.1021/ma400197c.
36. Mahmood N, Yuan Z, Schmidt J, Xu CC. Depolymerization of lignins and their applications for the preparation of polyols and rigid polyurethane foams: a review. Renew Sust Energ Rev. 2016;60:317–29. doi:10.1016/j.rser.2016.01.037.
37. Passoni V, Scarica C, Levi M, Turri S, Griffini G. Fractionation of industrial softwood kraft lignin: solvent selection as a tool for tailored material properties. ACS Sustain Chem Eng. 2016;4(4):2232–42. doi:10.1021/acssuschemeng.5b01722.
38. Duval A, Vilaplana F, Crestini C, Lawoko M. Solvent screening for the fractionation of industrial kraft lignin. Holzforschung. 2016;70(1):11–20. doi:10.1515/hf-2014-0346.
39. Tagami A, Gioia C, Lauberts M, Budnyak T, Moriana R, Lindström ME, et al. Solvent fractionation of softwood and hardwood kraft lignins for more efficient uses: compositional, structural, thermal, antioxidant and adsorption properties. Ind Crops Prod. 2019;129:123–34. doi:10.1016/j.indcrop.2018.11.067.
40. Jiang X, Savithri D, Du X, Pawar S, Jameel H, Chang HM, et al. Fractionation and characterization of kraft lignin by sequential precipitation with various organic solvents. ACS Sustain Chem Eng. 2017;5(1):835–42. doi:10.1021/acssuschemeng.6b02174.

41. Yu S, Wang M, Xie Y, Qian W, Bai Y, Feng Q. Lignin self-assembly and auto-adhesion for hydrophobic cellulose/lignin composite film fabrication. Int J Biol Macromol. 2023;233:123598. doi:10.1016/j.ijbiomac.2023.123598.
42. Ma Z, Li C, Fan H, Wan J, Luo Y, Li BG. Polyhydroxyurethanes (PHUs) derived from diphenolic acid and carbon dioxide and their application in solvent-and water-borne PHU coatings. Ind Eng Chem Res. 2017;56(47):14089–100. doi:10.1021/acs.iecr.7b04029.
43. Karaaslan MA, Cho M, Liu LY, Wang H, Renneckar S. Refining the properties of softwood kraft lignin with acetone: effect of solvent fractionation on the thermomechanical behavior of electrospun fibers. ACS Sustain Chem Eng. 2020;9(1):458–70. doi:10.1021/acssuschemeng.0c07634.
44. Liu LY, Cho M, Sathitsuksanoh N, Chowdhury S, Renneckar S. Uniform chemical functionality of technical lignin using ethylene carbonate for hydroxyethylation and subsequent greener esterification. ACS Sustain Chem Eng. 2018;6(9):12251–60. doi:10.1021/acssuschemeng.8b02649.
45. Glasser WG, Davé V, Frazier CE. Molecular weight distribution of (semi-) commercial lignin derivatives. J Wood Chem Technol. 1993;13(4):545–59. doi:10.1080/02773819308020533.
46. Mun JS, Pe III JA, Mun SP. Chemical characterization of kraft lignin prepared from mixed hardwoods. Molecules. 2021;26(16):4861. doi:10.3390/molecules26164861.
47. Konduri MK, Fatehi P. Production of water-soluble hardwood kraft lignin via sulfomethylation using formaldehyde and sodium sulfite. ACS Sustain Chem Eng. 2015;3(6):1172–82. doi:10.1021/acssuschemeng.5b00098.
48. Lourençon TV, Hansel FA, da Silva TA, Ramos LP, de Muniz GI, Magalhães WL. Hardwood and softwood kraft lignins fractionation by simple sequential acid precipitation. Sep Purif Technol. 2015;154:82–8. doi:10.1016/j.seppur.2015.09.015.
49. Zhu W. Equilibrium of lignin precipitation: the effects of ph, temperature, ion strength and wood origins (Master Thesis). Chalmers University of Technology: Sweden; 2013.
50. Wibowo ES, Park BD. The role of acetone-fractionated Kraft lignin molecular structure on surface adhesion to formaldehyde-based resins. Int J Biol Macromol. 2023;225:1449–61. doi:10.1016/j.ijbiomac.2022.11.202.
51. Li H, McDonald AG. Fractionation and characterization of industrial lignins. Ind Crops Prod. 2014;62:67–76. doi:10.1016/j.indcrop.2014.08.013.
52. Faix O. Classification of lignins from different botanical origins by FT-IR spectroscopy. Holzforschung. 1991;45:21–7. doi:10.1515/hfsg.1991.45.s1.21.
53. Silverstein RM, Bassler GC. Spectrometric identification of organic compounds. J Chem Educ. 1962;39(11):546–53. doi:10.1021/ed039p546.
54. Alinejad M, Henry C, Nikafshar S, Gondaliya A, Bagheri S, Chen N, et al. Lignin-based polyurethanes: opportunities for bio-based foams, elastomers, coatings and adhesives. Polym. 2019;11(7):1202. doi:10.3390/polym11071202.
55. Kim KH, Kim CS. Recent efforts to prevent undesirable reactions from fractionation to depolymerization of lignin: toward maximizing the value from lignin. Front Energy Res. 2018;6:92. doi:10.3389/fenrg.2018.00092.
56. Gigli M, Crestini C. Fractionation of industrial lignins: opportunities and challenges. Green Chem. 2020;22(15):4722–46. doi:10.1039/D0GC01606C.
57. Xu J, Li C, Dai L, Xu C, Zhong Y, Yu F, et al. Biomass fractionation and lignin fractionation towards lignin valorization. Chem Sus Chem. 2020;13(17):4284–95. doi:10.1002/cssc.202001491.
58. Crestini C, Lange H, Sette M, Argyropoulos DS. On the structure of softwood kraft lignin. Green Chem. 2017;19(17):4104–21. doi:10.1039/C7GC01812F.
59. Wibowo ES, Park BD. Chemical and thermal characteristics of ion-exchanged lignosulfonate. Molecules. 2023;28(6):2755. doi:10.3390/molecules28062755.
60. Abdelaziz OY, Meier S, Prothmann J, Turner C, Riisager A, Hulteberg CP. Oxidative depolymerisation of lignosulphonate lignin into low-molecular-weight products with Cu-Mn/δ-Al_2O_3. Top Catal. 2019;62:639–48. doi:10.1007/s11244-019-01146-5.

61. Ahvazi B, Cloutier E, Wojciechowicz O, Ngo TD. Lignin profiling: a guide for selecting appropriate lignins as precursors in biomaterials development. ACS Sustain Chem Eng. 2016;4(10):5090–105. doi:10.1021/acssuschemeng.6b00873.
62. Gutierrez L, Uribe L, Hernandez V, Vidal C, Mendonça RT. Assessment of the use of lignosulfonates to separate chalcopyrite and molybdenite by flotation. Powder Technol. 2020;359:216–25. doi:10.1016/j.powtec.2019.10.015.
63. Hemmilä V, Hosseinpourpia R, Adamopoulos S, Eceiza A. Characterization of wood-based industrial biorefinery lignosulfonates and supercritical water hydrolysis lignin. Waste Biomass Valori. 2020;11:5835–45. doi:10.1007/s12649-019-00878-5.
64. Vovk M, Sernek M. Aluminium trihydrate-filled poly(methyl methacrylate) (PMMA/ATH) waste powder utilization in wood-plastic composite boards bonded by MUF resin. BioResources. 2020;15(2):3252–69. doi:10.15376/biores.15.2.3252-3269.
65. Alonso E, Pothan LA, Ferreira A, Cordeiro N. Surface modification of banana fibers using organosilanes: an IGC insight. Cellul. 2019;26:3643–54. doi:10.1007/s10570-019-02329-9.
66. Lavoratti A, Zattera AJ, Amico SC. Mechanical and dynamic-mechanical properties of silane-treated graphite nanoplatelet/epoxy composites. J Appl Polym Sci. 2018;135(45):46724. doi:10.1002/app.46724.
67. Xi X, Wu Z, Pizzi A, Gerardin C, Lei H, Zhang B, et al. Non-isocyanate polyurethane adhesive from sucrose used for particleboard. Wood Sci Technol. 2019;53:393–405. doi:10.1007/s00226-019-01083-2.
68. Carré C, Bonnet L, Avérous L. Original biobased nonisocyanate polyurethanes: solvent- and catalyst-free synthesis, thermal properties and rheological behaviour. Rsc Adv. 2014;4(96):54018–25. doi:10.1039/C4RA09794G.
69. Saražin J, Poljanšek I, Pizzi A, Šernek M. Curing kinetics of tannin and lignin biobased adhesives determined by DSC and ABES. J Renew Mater. 2022;10(8):2117–31. doi:10.32604/jrm.2022.019602.
70. Cabrera IC, Berlioz S, Fahs A, Louarn G, Carriere P. Chemical functionalization of nano fibrillated cellulose by glycidyl silane coupling agents: a grafted silane network characterization study. Int J Biol Macromol. 2020;165:1773–82. doi:10.1016/j.ijbiomac.2020.10.045.